Use of Normalized Anomaly Fields to Anticipate Extreme Rainfall in the Mountains of Northern California

NORMAN W. JUNKER,* RICHARD H. GRUMM,+ ROBERT HART,# LANCE F. BOSART,@ KATHERINE M. BELL,& AND FRANK J. PEREIRA**

* *NOAA/NCEP/Hydrometeorological Prediction Center/I. M. Systems Group, Camp Springs, Maryland*
+ *NWS, State College, Pennsylvania*
# *Department of Meteorology, The Florida State University, Tallahassee, Florida*
@ *Department of Earth and Atmospheric Science, The University at Albany, State University of New York, Albany, New York*
& *NOAA/NCEP/Ocean Prediction Center, Camp Springs, Maryland*
** *NOAA/NCEP/Hydrometeorological Prediction Center, Camp Springs, Maryland*

(Manuscript received 31 January 2007, in final form 21 August 2007)

ABSTRACT

Extreme rainfall events contribute a large portion of wintertime precipitation to northern California. The motivations of this paper were to study the observed differences in the patterns between extreme and more commonly occurring lighter rainfall events, and to study whether anomaly fields might be used to discriminate between them. Daily (1200–1200 UTC) precipitation amounts were binned into three progressively heavier categories (12.5–50.0 mm, light; 50–100 mm, moderate; and >100 mm, heavy) in order to help identify the physical processes responsible for extreme precipitation in the Sierra Nevada range between 37.5° and 41.0°N.

The composite fields revealed marked differences between the synoptic patterns associated with the three different groups. The heavy composites showed a much stronger, larger-scale, and slower-moving negative geopotential height anomaly off the Pacific coast of Oregon and Washington than was revealed in either of the other two composites. The heavy rainfall events were also typically associated with an atmospheric river with anomalously high precipitable water (PW) and 850-hPa moisture flux (MF) within it. The standardized PW and MF anomalies associated with the heavy grouping were higher and were slower moving than in either of the lighter bins.

Three multiday heavy rainfall events were closely examined in order to ascertain whether anomaly patterns could provide forecast utility. Each of the multiday extreme rainfall events investigated was associated with atmospheric rivers that contained highly anomalous 850-hPa MF and PW within it. Each case was also associated with an unusually intense negative geopotential height anomaly that was similarly located off of the west coast of the United States. The similarities in the anomaly pattern among the three multiday extreme events suggest that standardized anomalies might be useful in predicting extreme multiday rainfall events in the northern Sierra range.

1. Introduction

Cool season precipitation is the major source of the water supply for California. Extreme precipitation events contribute a large fraction of the total cool season precipitation to California (Cayan and Riddle 1993) and have a significant sociological and economic impact (Baird and Robles 1997; Washburn 2003).

Accurate forecasts of extreme rainfall events and their associated runoff would allow for the advanced release of water from dams, thereby reducing the damage from floods. However, a direct trade-off exists between using precipitation forecasts to improve flood protection and the possibility of having a negative impact on water management. For example, if water is released from the reservoir based on a poor precipitation forecast, the reduced storage might then make it difficult to meet water demands during the subsequent summer. Therefore, improved methods for assessing the probability of extreme precipitation over northern California are needed (Faber 2003).

Corresponding author address: Norman W. Junker, NOAA Science Center, Hydrometeorological Prediction Center, Rm. 410, 5200 Auth Rd., Camp Springs, MD 20746.
E-mail: norman.w.junker@noaa.gov

DOI: 10.1175/2007WAF2007013.1

© 2008 American Meteorological Society

Many of the cold season extreme rainfall events in northern California have similar synoptic patterns. For example, Maddox et al. (1980) noted type III western flash flood events occurred when strong synoptic weather systems produced moist low-level flow that interacted with the mountains. Strobin and Reynolds (1995) have also discussed the typical synoptic type pattern associated with heavy rainfall events in northern California and developed a criteria checklist to aid in forecasting this type of event. More recently, Reynolds (1996) pointed out the similarities in the synoptic patterns for three major rainstorms during 1995. Each was associated with a strong synoptic-scale system that helped produce strong onshore flow. Pandey et al. (1999) noticed that a strong negative height anomaly to the northwest of California was associated with the 20 heaviest precipitation cases found over the Sierra Nevada during the period 1948–88.

Grumm and Hart (2001a) found that significant negative departures (greater than 3σ) from normal in the u component of the 850-hPa wind (indicative of easterly winds) were present in the model forecasts for several flash flood events over the middle Atlantic region. More recently, Grumm et al. (2002) examined a large group of heavy rainfall cases distributed across the country and noted that there appeared to be regional characteristics to the synoptic-scale patterns and associated height, wind, and moisture anomaly fields during these events. In this paper, we attempt to build upon these earlier studies and show how unusually large departures from normal in various meteorological parameters might be used as a tool for predicting extreme rainfall days in northern California.

2. Methodology

The National Centers for Environmental Prediction (NCEP) Hydrometeorological Prediction Center's (HPC) precipitation analyses as described in McDonald et al. (2000) and Junker et al. (2002) were used to detect days in which greater than 0.50 in. of liquid equivalent precipitation was analyzed in the Sierra Nevada range between 37.5° and 41.0°N. The 24-h precipitation analyses verify at 1200 UTC. Note that the smallest area analyzed on any of these maps is approximately 41 km^2. The precipitation days were binned into the following categories: light, between 12.7 and 50 mm (0.50–2.00 in.); moderate, between 50 and 100 mm (2.00–4.00 in.); and heavy, greater than 100 mm (4.00 in.). Composites for each category of precipitation were then developed in the hopes of identifying fields that might be useful to forecasters trying to predict precipitation potential over Sierra Nevada range. The bulk of the heavy rainfall days occurred between late fall and early spring; virtually no events were observed during the summer season.

For each day used in any of the composites, the mean sea level pressure, 700- and 500-hPa geopotential height, precipitable water (PW), 850- and 700-hPa moisture flux (MF), and u and v components of the wind analyses were examined at $T + 00$ (the beginning of the period) to its end 24 h later ($T + 24$). Gridded fields for these times were then compared to the daily climatological means from the 30-yr period spanning 1961–90 in a method similar to that described by Grumm and Hart (2001b) and Hart and Grumm (2000). The gridded data were retrieved from the NCEP–National Center for Atmospheric Research (NCAR) reanalysis project (Kalnay et al. 1996; Kistler et al. 2001). The dataset has 2.5° × 2.5° grid spacing at 17 pressure levels.

One drawback of using 24-h precipitation days to build the composites, rather than basing the composites on the total event, is that the event may not end at $T + 24$; when that occurs, $T + 24$ may become the $T + 00$ for the next day. This can result in composites being less "clean" than one might hope. However, determining the exact starting time and ending time of multiday events also can be problematic as precipitation along the West Coast often comes as a result of several consecutive storms with small breaks between them. Without adequate satellite coverage or hourly precipitation data, the starting and ending times can be difficult to determine. These additional data were not readily available. Despite the shortcomings of using the 24-h observed precipitation to classify the precipitation categories for the composites, the authors believe the differences in the normalized anomalies found between the heavy, moderate, and light composites are real, and that the most extreme rainfall events typically have higher normalized anomalies than those typically associated with light to moderate events.

Moisture flux in this article is defined as the vector composition of the product of the specific humidity and the u and v components of the wind at each point. The anomalies and normalized anomalies of MF are based on the departures from the mean of the magnitude of the total moisture flux.

Departures from normal for each grid point were obtained by comparing the selected meteorological field or parameter with the 21-day mean (from the 30-yr NCEP–NCAR reanalysis), centered on the day being investigated. Standard deviations were also calculated using the 21-day running mean. The Grid Analysis and Display System (GRADS; information online at http://grads.iges.org/grads/) was used to compute and plot the means, anomaly fields, and standard deviations

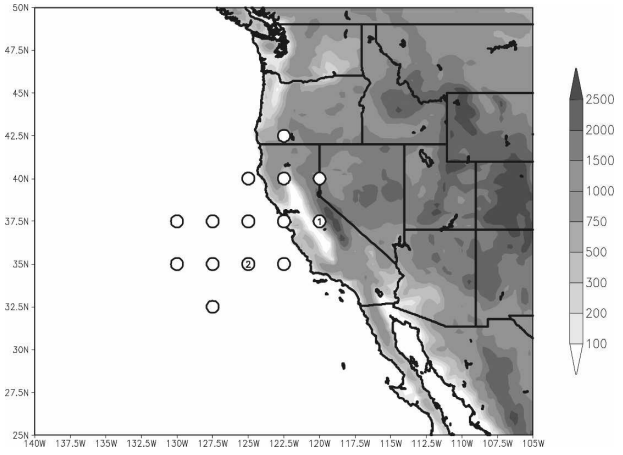

FIG. 1. Points used to calculate the percentage of the total distribution for normalized anomalies of PW and 850-hPa magnitude of MF. The normalized anomalies of PW, the u and v components of the wind, and the magnitude of the MF and of the component of the MF normal to the mountains were recorded for points 1 and 2 to determine the correlations with the maximum analyzed rainfall contour in the Sierra Nevada range. Terrain is shaded with the legend for the elevation (m) shown at right.

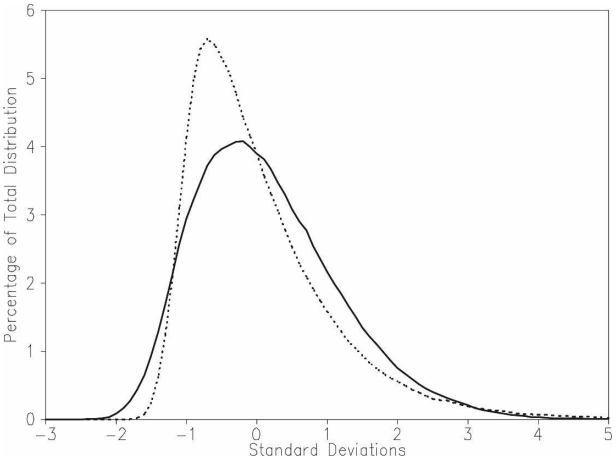

FIG. 2. Histogram showing the percentage of the total distribution for the normalized anomalies of PW (solid line) and the magnitude of the 850-hPa MF (dotted line).

of PW, as well as the 700- and 850-hPa heights, MF, and winds.

Hart and Grumm (2001) used normalized departures from climatology to objectively rank synoptic-scale events. We are attempting to build on their research by investigating whether normalized anomalies can be used to help identify when a significant rainfall event is likely to occur in the northern portions of the Sierra Nevada range.

The normalized departure of any meteorological variable can be defined by

$$N = (X - \mu)/\sigma, \tag{1}$$

where X is the value of the variable (e.g., 500-hPa height, u and v components of the 850-hPa wind, or MF, etc.), μ is the daily mean value (based on the 21-day running mean) for that grid point, and σ is the standard deviation (based on the 21-day running mean) for each grid point.

Finally, the normalized anomalies of the 850- and 700-hPa moisture flux, u and v components of the wind at the same levels, and the PW value were recorded for the points 37.5°N, 120°W and 35°N, 125°W (in Fig. 1) at 1200 UTC (the beginning of the period), 0000 UTC (the middle of the period), and 1200 UTC (the end of the 24-h period). The components of the moisture flux perpendicular to the Sierra range (a wind of 240° was considered perpendicular to the range) at 700 and 850 hPa were also recorded for points 1 and 2. A simple arithmetic average of the normalized anomaly at that point was then calculated for the 24-h period in which the observed precipitation was measured. The value of R square was then calculated for the averaged normalized anomalies and the maximum observed isohyet that was noted in the Sierra Nevada range between 37.5° and 41.0°N for 163 days on which a maximum analyzed rainfall of at least 12.5 mm occurred. The various R-square values were calculated using the highest observed precipitation total analyzed on the HPC analysis based on the following categories: 12.5–25 mm (0.50–1.00 in.), 25–50 mm (1.00–2.00 in.), 50–75 mm (2.00–3.00 in.), 75–100 mm (3.00–4.00 in.), 100–125 (4.00–5.00 in.), and greater than 175 mm (6.00 in.). Readers should note that this final dataset was also from the HPC analyses but included only events that had rainfall amounts greater than 12.5 mm (0.50 in.) of rainfall. Therefore, the correlations found were conditional on at least 12.5 mm of rainfall actually being observed.

The normalized anomalies of the various parameters for 0000 and 1200 UTC each day in the 10-yr climatology were also entered into a relational database to evaluate whether these fields could be used to discriminate between days when at least 100 mm (4.00 in.) of rain fell over northern California from days with less rainfall, and to find out how often various combinations of high anomalies occurred.

Finally, a histogram was developed to show the distribution of the 850-hPa MF and PW anomalies for all of the points in Fig. 1. Notice that the frequency of events with standard deviations of greater than three is still quite small despite the skewness of the curves (Fig. 2).

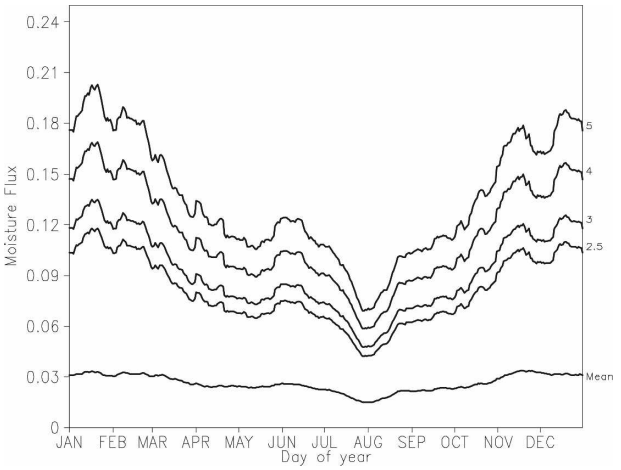

FIG. 3. Plot of the annual cycle of the mean magnitude of MF (interval = 0.03 m s^{-1}) and the mean magnitude of MF associated with the normalized anomalies of 2.5, 3, 4, and 5 std dev at 37.5°N, 125°W.

3. Results

All of the heavy precipitation days in California that were of sufficient scale to be analyzed on the HPC maps occurred between mid-October and mid-May, with the majority occurring in November–March. No events were noted during the warm season period (June–September). The cool season maximum and warm season minimum in the frequency of heavy rainfall events in California appeared to be modulated by the seasonal variations in the magnitude of the MF (Fig. 3). Pandey et al. (1999) have noted that the MF was typically higher during days with greater than average rainfall in the Sierra Nevada range. In this study, the magnitude of the MF associated with various normalized anomalies during the November–March period was much higher than the MF associated with the corresponding normalized anomalies for the June–September period (Fig. 3). This helps explain the cool season extreme rainfall frequency maximum; MF is typically significantly higher during the cold season than during the warm season.

a. Investigation of the normalized anomaly fields associated with the mass and wind field composites

The 700-hPa height pattern for the three different rainfall categories was markedly different (Fig. 4). The composites associated with each rainfall category revealed a trough off the West Coast that is associated with an area of below normal heights (Fig. 5) off the Pacific Northwest coast. However, a comparison between the troughs at $T + 00$ (Figs. 4a–c) indicated that the trough is stronger and larger in scale at the onset of the heavy cases than for the moderate or lighter ones. The position of the mean short-wave ridge upstream from the trough was also farther west during heavy rainfall events than during the moderate or light ones. Also, the trough was less progressive for the heavy events compared to the two lighter categories.

The normalized anomaly pattern at 700 hPa (Fig. 5) for the heavy events was very similar to the anomaly pattern found by Pandey et al. (1999) for 20 heavy rainfall events that occurred in the northern Sierra Nevada. An area of anomalously low heights was located off the Pacific Northwest coast with a weaker positive anomaly located to its southeast near Baja. The composite of the moderate events also exhibited this dipole. The resulting gradient implies that a long fetch of southwesterly geostrophic winds is present during the heavy events. The magnitude of the negative anomaly was higher for the heavy events with the negative anomaly extending much farther to the south and west than in either the moderate or light event composites. Such a southwestward extension would likely allow for more tropical moisture to be pulled northeastward. The orientation of the southwestern extension of the negative anomaly in the heavy rainfall composite suggests that such cases are more likely to maintain a positive tilt than in the typical light to moderate events. Pandey et al. (1999) also found a similar orientation and southwestward extension of the below normal heights.

A comparison of the normalized anomaly patterns at $T + 00$ versus $T + 24$ (Fig. 5) indicates that the negative anomaly was less progressive during the heavy events than for the moderate ones. Note that the composite mean 700-hPa anomaly center at $T + 24$ was located farther west for the heavy events than during the moderate ones. The magnitude of the anomaly changed little during the 24 h for the heavy cases but weakened on the moderate composite as the anomaly center shifted into the coast. During the light rainfall events, the magnitude of the anomaly was weaker at all times than in either the heavy or moderate composites; in addition, the anomaly center was more progressive. Therefore, the strength of the geopotential height gradient between the two dipoles, the orientation of the 700-hPa trough, and the slow movement of the negative height anomaly center appear to be important clues about the potential for heavy rainfall. The differences in the implied geopotential height gradients between the three groups are not surprising. James and Houze (2005) have noted that all of the features of the orographically enhanced precipitation were more pronounced when the 500–700-hPa flow was strong and when the low-level jet was strong.

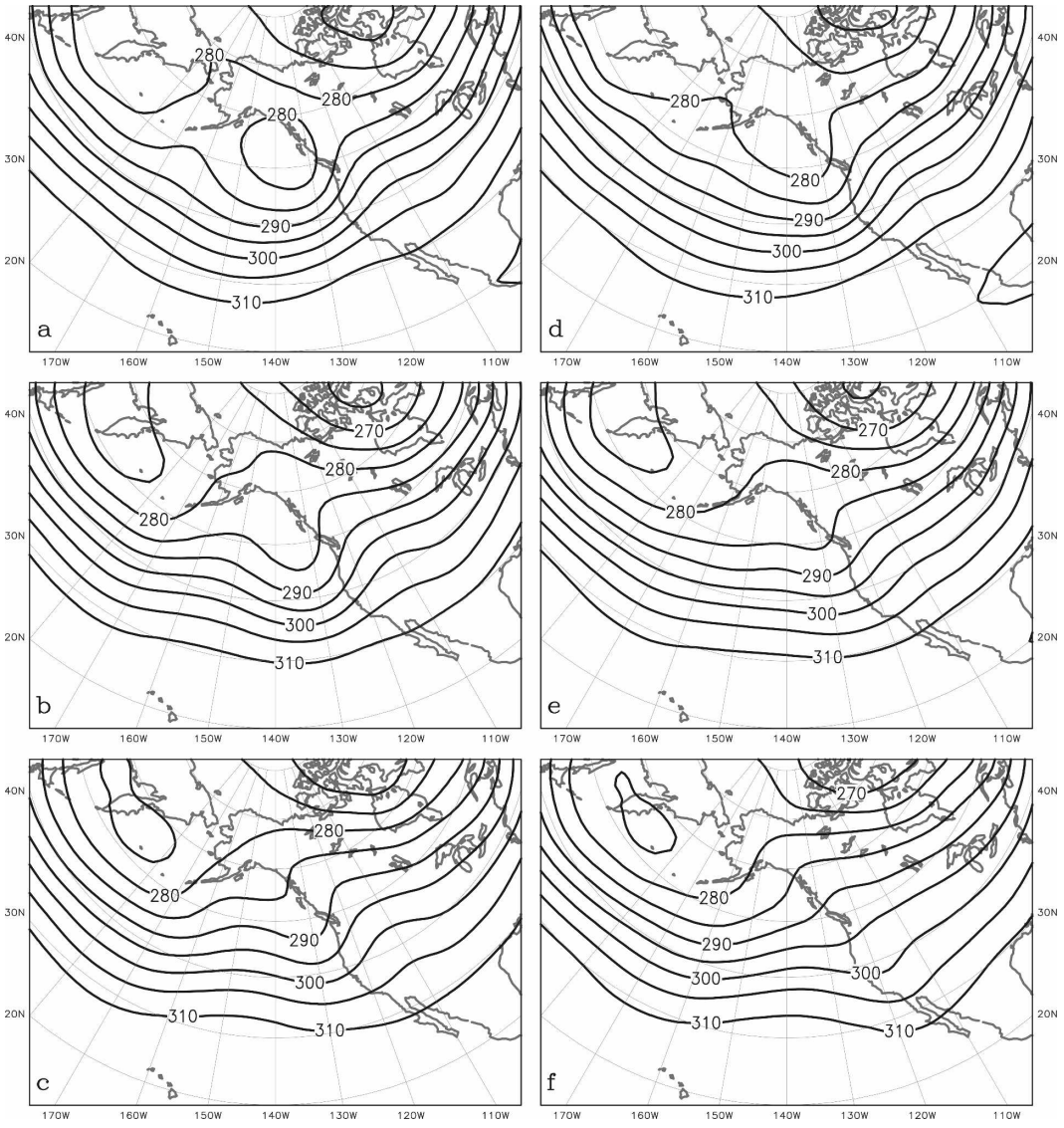

FIG. 4. Composite mean 700-hPa height field for $T + 00$ (the time of the beginning of the period of rainfall) for (a) heavy, (b) moderate, and (c) light rainfall days; and $T + 24$ (the end of the period) for (d) heavy, (e) moderate, and (f) light rainfall days. Contour interval = 5 dam and latitude and longitude intervals are 10°.

The composite mean sea level pressure (Fig. 6) at $T + 00$ for heavy rainfall events when compared to those from the other two categories indicates that the low is typically stronger during heavy rainfall events than during the typical moderate or light event. The composite means of the moderate and light events both show a surface trough located between 125° and 130°W. The orientation of the isobars west of the trough implies that the geostrophic winds west of 130°W have a west-northwesterly component for the two lighter categories. By contrast, the geostrophic winds implied by the composite mean of the heavy events are almost zonal between 27° and 36°N, with a slight component from the south; the geostrophic winds in heavy rainfall events would probably be more parallel to the front than for either of the lighter categories, suggesting that the front might be slower moving.

For the heavy events, the normalized anomaly pattern for mean sea level composites (not shown) for the different categories exhibit many of the same differences found in the 700-hPa composite mean anomaly analyses. The negative anomaly located off the Pacific Northwest was stronger in the heavy composite than in the moderate or light ones and it extended farther to the south and west.

The normalized height anomaly pattern for the

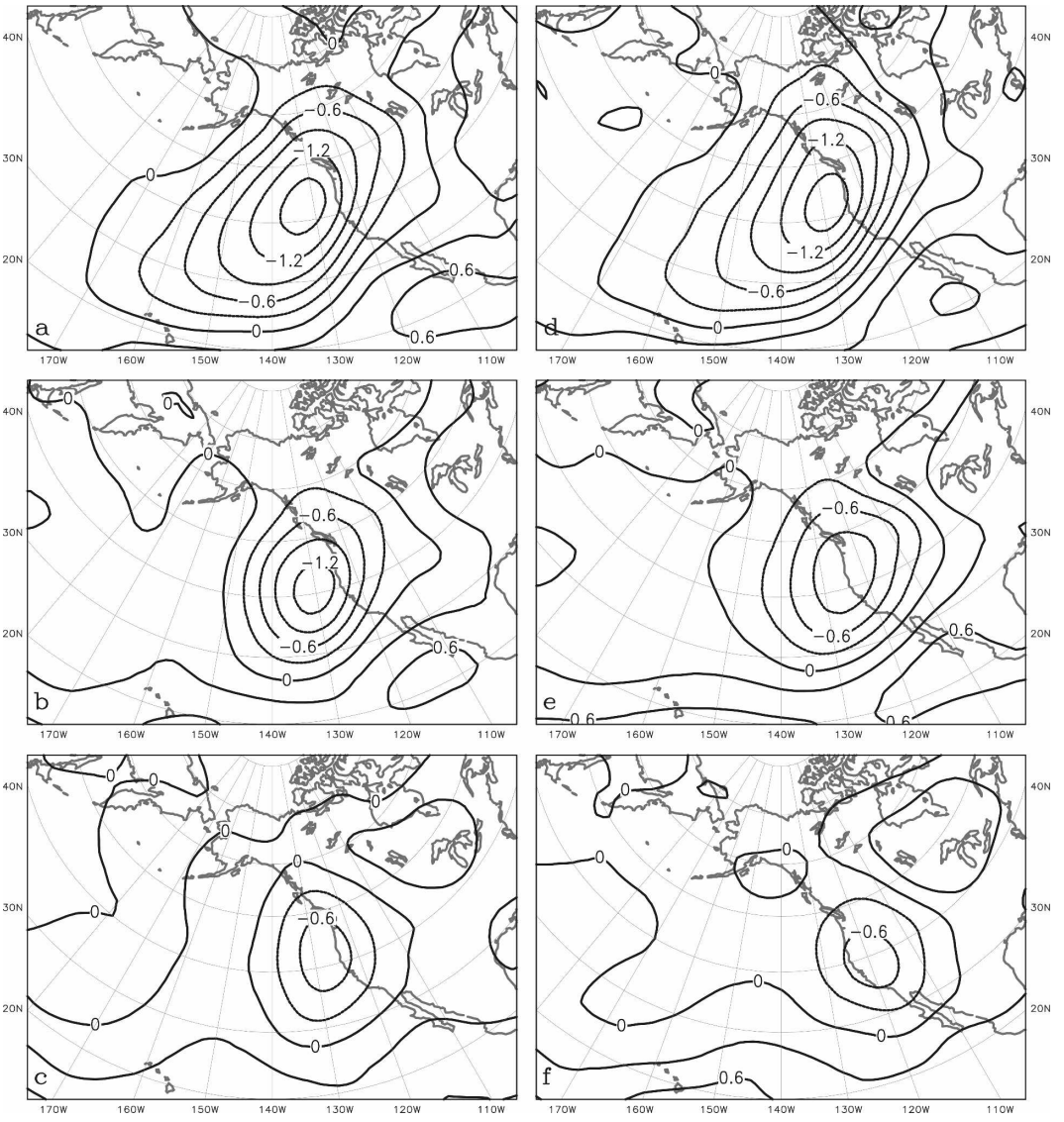

FIG. 5. Same as in Fig. 4, but for the normalized 700-hPa geopotential height anomalies. The contour interval is 0.3σ.

500-hPa heavy day composite at $T + 00$ (Fig. 7a) has a dipole pattern similar to the corresponding pattern on the 700-hPa composite. The juxtaposition of the strong negative anomaly off the Pacific Northwest coast and the positive couplet to its southeast suggest the presence of stronger than normal geostrophic winds as well as a stronger than normal jet to the south of the negative geopotential height anomaly maximum. The 500-hPa heavy rainfall composite also reveals a weak positive height anomaly near Alaska. Strobin and Reynolds (1995) have also noted a similar 500-hPa pattern and have suggested that a blocking ridge near Alaska is often present to the northwest of the positive–negative anomaly couplet that helps provide the strong gradient associated with the enhanced southwesterly flow into the California coast.

The positive–negative anomaly couplet that extends from the surface to 500 hPa implies that stronger than normal southwesterly geostrophic winds are present through a deep layer. Lackmann and Gyakum (1999) found similar mean sea level and 500-hPa height anomalies and a similar couplet associated with heavy cold season precipitation events in the northwestern United States. They noted that during the Pacific Northwest cases, this pattern of anomalies often results in warm, moist subtropical air from near the Hawaiian Islands being transported northeastward into Washington and Oregon, and noted that

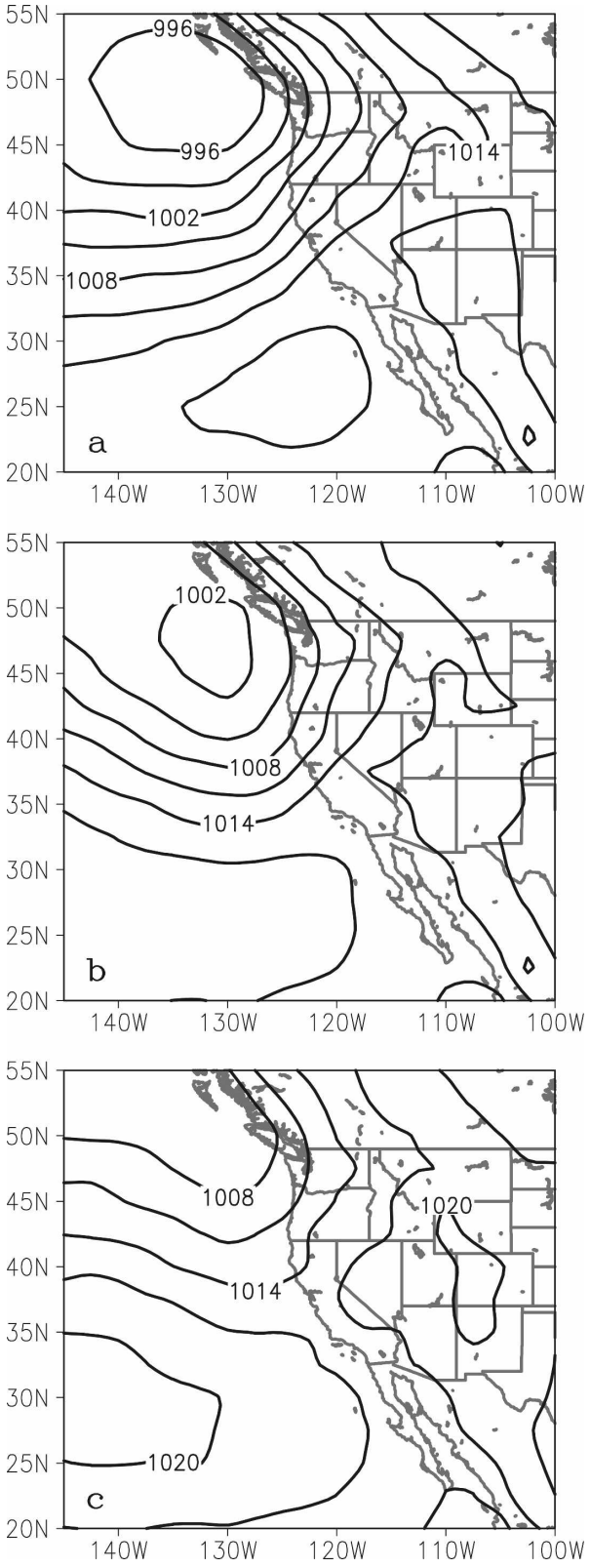

FIG. 6. Composite mean sea level pressure at $T + 00$ for (a) heavy, (b) moderate, and (c) light rainfall days. Contour interval is 3 hPa.

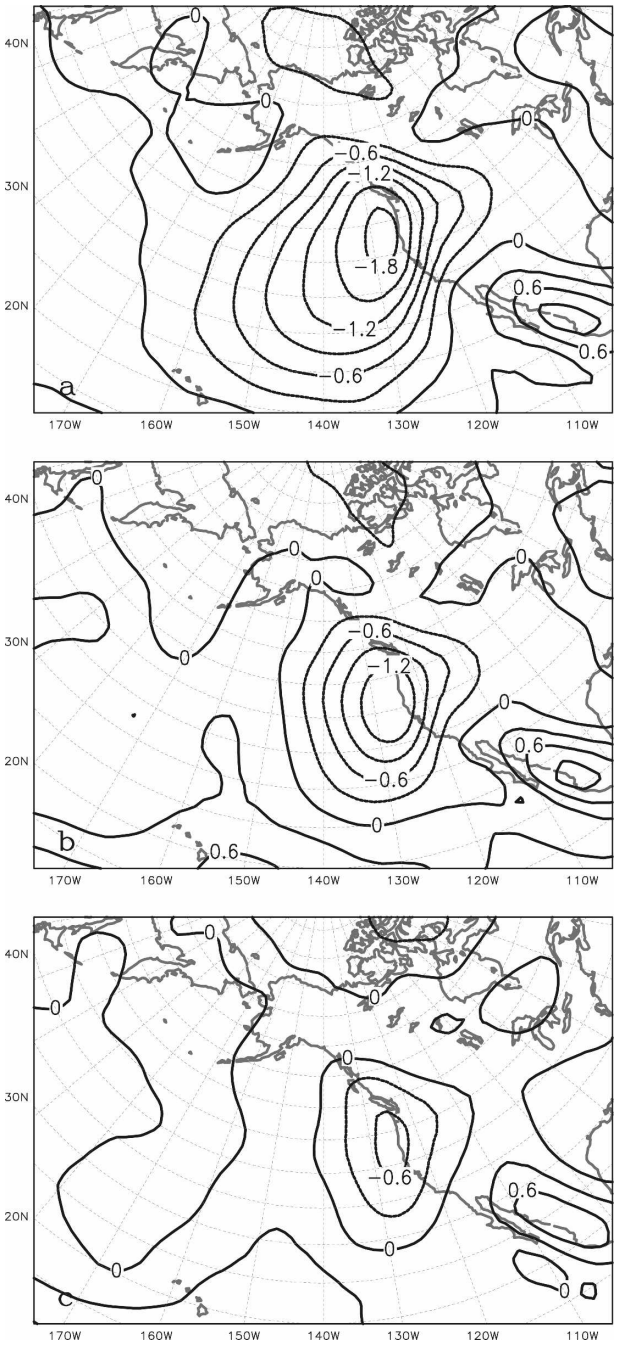

FIG. 7. Composite mean normalized anomaly of 500-hPa heights for $T + 00$ for (a) heavy and (b) moderate rainfall events. Contour interval is 0.3σ. Latitude and longitude intervals are 10°.

such flow has sometimes been called the "pineapple express."

The location of the center of the negative anomaly at 500 hPa was similar for the heavy and moderate groupings at the onset of the event (Figs. 7a and 7b). However, there were subtle differences in the anomaly pat-

terns between the two groupings. The area with a negative height anomaly was larger for the heavy grouping than was found in the moderate rainfall composite (Figs. 7a and 7b). The negative anomaly also extended farther to the southwest, suggesting that the troughs associated with heavy events typically have a more of positive tilt than do the moderate events and also have a larger scale. The anomaly center on the heavy rainfall event composite was also less progressive than for the moderate one (not shown). The anomaly for the latter weakened as it shifted eastward during the 24-h period (not shown).

A number of researchers have studied the role of the wind and topography in the distribution of rainfall over complex terrain (Alpert 1986; Alpert and Shafir 1991; Rhea 1978; Neiman et al. 2002). Based on the strong link found by Neiman et al. (2002) between the magnitude of the low-level jet and rainfall intensity, the magnitudes of the u and v components of the 850-hPa winds might have utility in diagnosing which rainfall events have the potential for being extreme. Neiman et al. found a high correlation between rainfall rates in the coastal ranges of California and the winds just below the mountaintops, typically below 850 hPa. That study's results encouraged us to explore the u- and v-component wind anomalies along and upstream from the Sierra Nevada range.

The normalized anomalies of the u component of the 850-hPa wind indicate that there were anomalous westerly u components of the wind present at $T + 00$ for all three categories of rainfall (Figs. 8a–c). However, the magnitude of the anomaly was much greater on the heavy and moderate composites than on the light one. Also, the area of the 1.2σ or greater normalized anomaly extended much farther west on the heavy rainfall composite than on the moderate bin composite at $T + 00$. The normalized anomaly of the u component of the wind increases and the anomaly center remains off the coast in the heavy rainfall composite at $T + 24$ (Fig. 8d). By contrast, the anomaly center in the moderate rainfall composite (Fig. 8e) shifts to the coast in response to its more progressive short wave. The anomaly center of the light rainfall grouping actually shifts southeastward during the 24-h period (cf. Figs. 8c and 8f).

There was a significant difference in the v components of the wind (not shown) between the three groupings at $T + 00$. Anomalously strong southerly winds at 850 hPa at 27°N extended to 145°W in the heavy rainfall event composite but only to 135°W for the moderate composite. The area of the more than 1.2σ above normal southerly wind component extended westward from the coast to almost 135°W on the heavy rainfall composite compared to 123°W on the moderate composite.

The anomalously strong southerly component of the winds in the heavy rainfall composite may explain the warm temperature anomalies that a number of researches have noted during heavy rainfall events along the west coast of the United States. Lackmann and Gyakum (1999), in their study of heavy rainfall events of the northwestern United States, also detected a warm anomaly. Pandey et al. (1999) found a similar warm anomaly associated with his composite of 50.8-mm events in the Sierra Nevada. At 850, 700, and 500 hPa, a similar positive temperature anomaly was noted in our composite of heavy events at $T + 00$ (not shown). This anomaly shifted eastward across the southwest and extended into the western high plains by $T + 24$. Lackmann and Gyakum have suggested that pineapple express cases may be accompanied by widespread warming. Our results support their speculation that pineapple express events bring anomalously warm temperatures into the west.

The normalized v-component wind anomalies at 850 hPa are stronger, and positive anomalies stretch farther south and west on the heavy composite than on the composites for either of the lighter thresholds (not shown). The southwestward extension of the anomalously high southerly v-component winds at 850 hPa during the heavier events probably helps explain why there were also greater moisture flux and PW anomalies present offshore during the heavy events than during the more moderate events as the southerly winds could more easily tap the deep subtropical moisture.

b. Investigation of the normalized anomaly fields of PW and MF

Pandey et al. (1999) have noted higher observed MF at Oakland, California, during events that produced 50 mm of liquid equivalent precipitation over the Sierra Nevada than in events that produced 25 mm, with the maximum MF near or just below 800 hPa. Zhu and Newell (1998) have documented that greater than 90% of the total meridional moisture transport at midlatitudes is contained within narrow plumes of horizontal moisture that they define as atmospheric rivers that cover less than 10% of the total hemispheric circumference. Ralph et al. (2004) have noted that within these rivers the horizontal water vapor flux is concentrated at the lower levels of the atmosphere in a narrow region in advance of the cold front where there is a combination of strong winds and large water vapor content. In another study, Ralph et al. (2005), using a 17-case composite of the mean vertical profiles of the wind speed and MF within atmospheric rivers, indicated that the

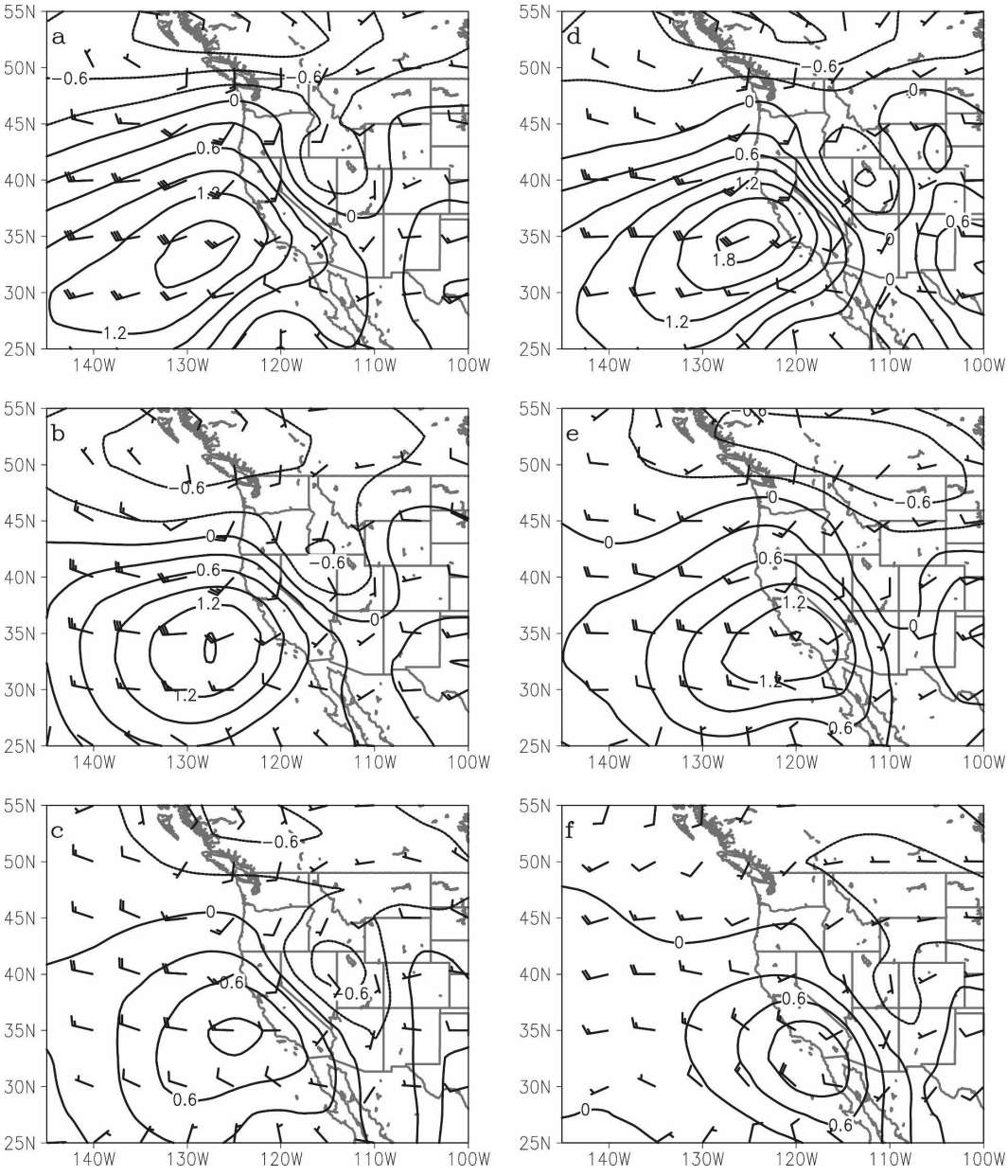

FIG. 8. Same as in Fig. 4, but for composite mean 850-hPa total wind (flags are 50 kt, barbs are 10 kt, and half barbs are 5 kt) and the normalized anomaly of the u component of the wind. Contour interval is 0.3σ.

low-level jet (LLJ) is typically located below 850 hPa and that the maximum MF is located near the level of the LLJ with MF steadily decreasing above that level. In an even more recent study, Ralph et al. (2006) documented that seven floods on the Russian River in California were associated with landfalling atmospheric rivers.

Neiman et al. (2008) have noted that atmospheric rivers and their associated enhanced low-level moisture transport have a significant impact on the weather along the West Coast from northern Mexico northward to Washington and contribute significantly to precipitation and flooding in western North America. This same study also found that the NCEP–NCAR reanalysis accurately captured the orientation of integrated water vapor plumes that were observed by the Special Sensor Microwave Imager (SSM/I). These studies imply that composites of 850-hPa MF, PW, and the normalized anomalies of both these fields might provide clues to the rainfall potential during extreme rainfall events.

There were differences in the normalized anomaly

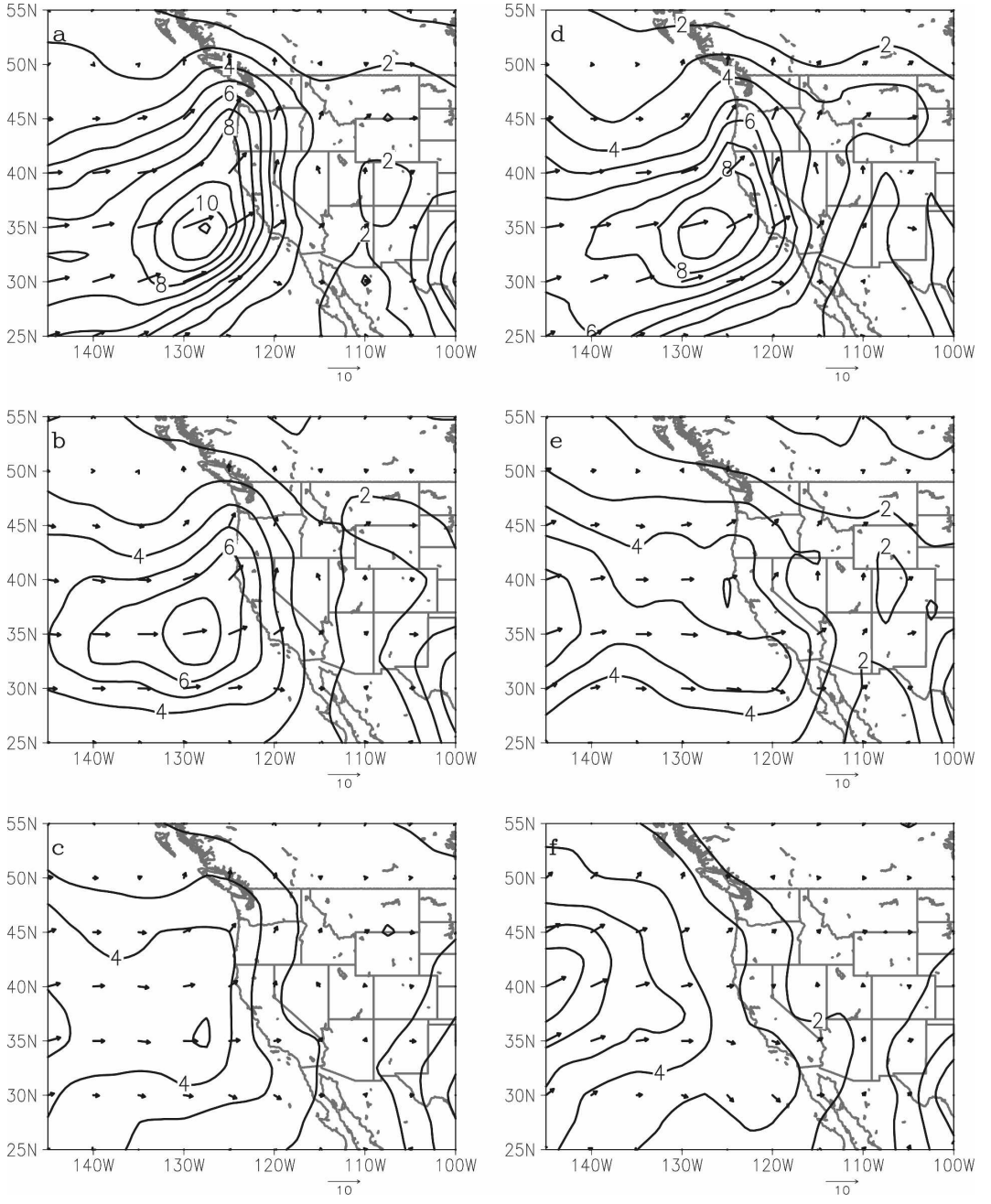

FIG. 9. Same as in Fig. 4, but for composite mean 850-hPa total MF (arrows show direction and are scaled as shown at the bottom of the figure) and magnitude of total MF (10^{-2} m s^{-1}).

patterns of the 850-hPa MF between the three rainfall groups at $T + 00$ that became more pronounced by $T + 24$. The location of the highest moisture flux and the orientation of the axis of the strongest moisture flux are very similar in the composite mean analyses for the heavy (Fig. 9a), moderate (Fig. 9b), and light (Fig. 9c) events at $T + 00$. However, the MF magnitude is greater for the heavy events than for the moderate ones, with the latter having significantly higher values than the light event composite. The axis of the strongest moisture flux presses southward much more slowly during the heavy events than during the moderate and light events (Fig. 9). At $T + 24$, the magnitude of the moisture flux is almost twice as strong at Oakland in the heavy composite than in the moderate one. This is consistent with the findings in the Pandey et al. (1999)

study, which showed the moisture flux at Oakland was higher during 50-mm or greater events than during 25-mm or greater ones.

The more southward push of the moisture flux axis in the moderate composite than in the heavy one (cf. Figs. 9d and 9e) is probably related to its more progressive trough. Also, the slight northerly component to the 850-hPa winds (Fig. 8) that develops behind the short wave would tend to cut off any tap into the subtropical moisture in the moderate composite. Therefore, the moisture associated with atmospheric rivers during moderate rainfall events decreases more quickly than that during heavy events. In essence, the atmospheric river becomes pinched off from its moisture source in the moderate composite.

The normalized anomalies of the magnitude of the 850-hPa MF were greater at $T + 00$ and $T + 24$ for the heavy events than for any other field investigated, and are significantly higher than the normalized moisture flux anomalies for the moderate or light groupings (Fig. 10). The differences in the mean 850-hPa MF and MF anomalies between the three groupings suggest that the structures of the atmospheric rivers during each type of event may be different and that such rivers may play little or no role during most light events. Slow-moving atmospheric rivers impinging upon the coast of California, however, appear to play a major role in the heavy events in the Sierra Nevada range, implying that the role of atmospheric rivers in producing heavy rainfall over the mountains of the West is not confined to the coastal ranges. The striking difference in the composites of the three categories supports the contention that normalized 850-hPa MF anomalies might be a useful tool in forecasting heavy rainfall events.

Ferraro et al. (1998) noted that moisture plumes of high PW (atmospheric rivers) are often associated with heavy rainfall events. Neiman et al. (2008) have suggested that wintertime PW plumes within atmospheric rivers have a minimum core value greater than 2 cm, and that those plumes with coherent regions of PW greater than 3 cm within 1000 km of the coast be classified as strong plumes. The composite mean PW and normalized PW anomaly fields support the idea that slow-moving atmospheric rivers are usually associated with heavy events and that light events are usually not associated with atmospheric rivers (Fig. 11). The composite mean PW plot suggests that atmospheric rivers or moisture plumes are associated with the moderate and heavy rainfall days but not the light ones. The location of the river is almost identical at $T + 00$ for the moderate and heavy events. However, the mean PW within the plume is higher in the heavy composite than in the moderate event composite (cf. Figs. 11a and 11b). Our findings are similar to the results found in the Neiman et al. study; rainfall associated with strong moisture plumes was greater than was typically found during days when a weaker plume was impinging on the coast.

The axis of highest PW shifts southward much more quickly in the moderate event composite than in the heavy one (Fig. 11), which is probably due to the faster eastward movement of the short wave into the coast. The composites for the heavy events show that these atmospheric rivers or plumes play an important role during extreme cold season rainfall events in northern California, and that these plumes can be identified using anomalies. Comparing the composite mean-normalized PW anomalies between the heavier and moderate lighter events, we can see that there are differences in the moisture within atmospheric rivers.

A comparison of the normalized anomalies for 850-hPa moisture flux and PW at $T + 00$ and $T + 24$ for the different rainfall categories in Figs. 10 and 12 with the composite mean and anomalous 700-hPa height fields in Fig. 5 reveals that higher normalized MF and PW anomalies in the heavy rainfall grouping are usually associated with 700-hPa troughs having larger spatial scales than during the lighter rainfall days. In addition, the midlevel and upper-level troughs (not shown) are broader and the associated upper-level jets (not shown) are stronger in the heaviest rainfall category than for either of the lighter categories. These findings indicate that upper-level disturbances of larger scale and wavelength are more likely to be associated with relatively slow-moving atmospheric rivers than faster-moving, shorter-wavelength upper-level disturbances. These observed differences are also consistent with Rossby wave theory (e.g., Holton 2004), in which the phase speed of the Rossby waves varies inversely as the wavelength squared.

The differences between the scales and magnitudes of the normalized anomalies between the different categories imply that model plots of normalized anomalies might have utility in identifying the potential for a heavy rainfall event.

c. Investigation of the normalized anomaly patterns during a multiday extreme rainfall event

Selected anomaly fields were examined for the multiday rainfall event of 31 December 1996–2 January 1997. This event produced major flooding or flash flooding in northern California (and prompted a federal disaster declaration). The New Year's flood of 1997 caused nearly $2 billion in property damage and forced over 100 000 people from their homes (Baird and Robles 1997). The case is not examined in the detail necessary to diagnose the exact mechanisms that

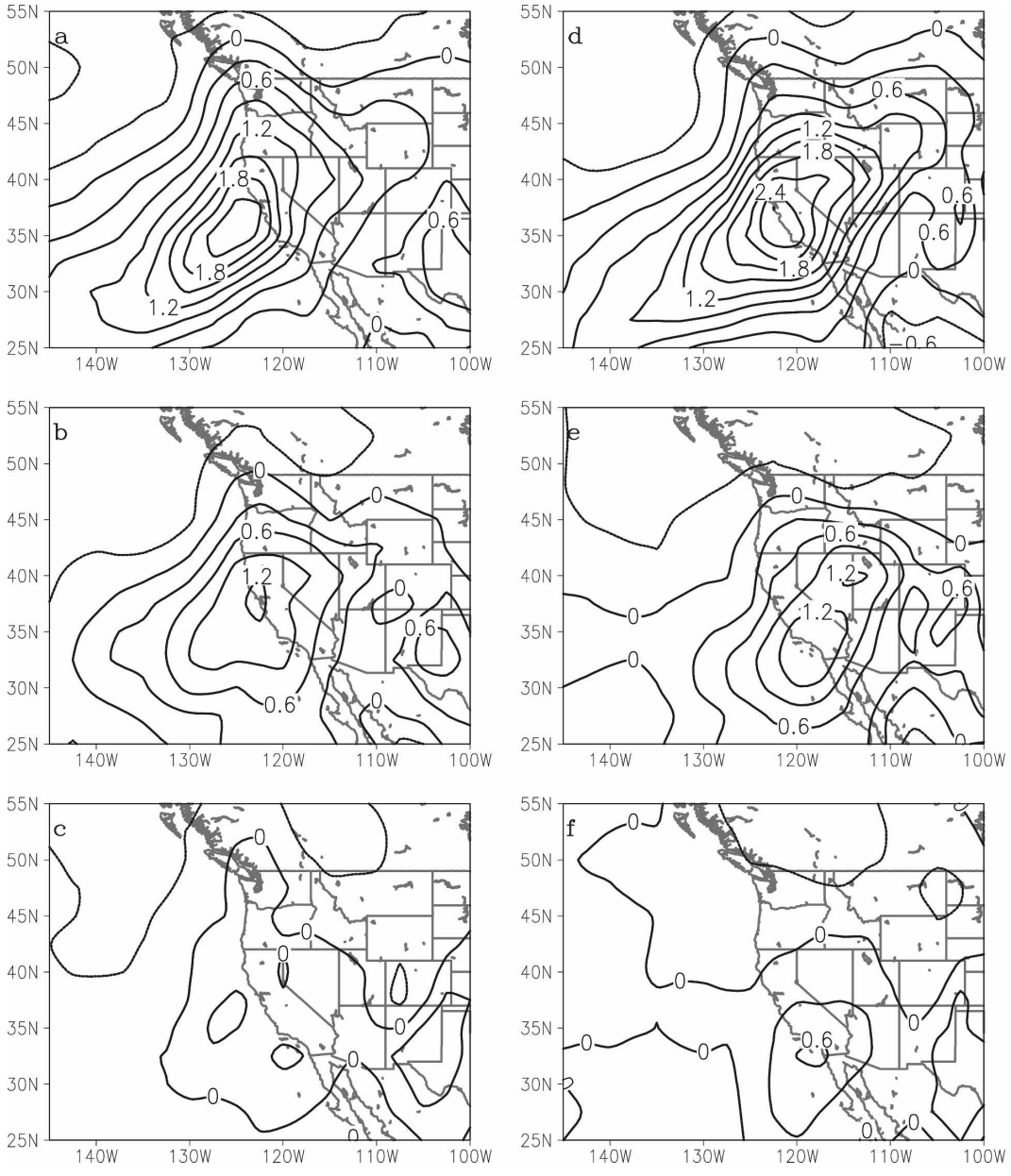

FIG. 10. Same as in Fig. 4, but for the composite mean normalized anomaly field of the magnitude of the total MF (contour interval is 0.3σ) at 850 hPa.

caused the extremely heavy rainfall; rather, the review of the case is meant to highlight the anomalous synoptic pattern. Two additional multiday heavy rainfall events that were associated with flooding and flash flooding and federal disaster declarations (9–11 January 1995 and 8–11 March 1995; Army Corps of Engineers 1999) were investigated. These two cases had anomaly patterns of similar magnitude and scale to the 31 December 1996–2 January 1997 case for most of the fields under review. These two additional cases will be touched upon, but figures illustrating the anomaly patterns will not be shown in this article due to space constraints.

A highly anomalous 700-hPa trough with height anomalies of more than 3σ below normal (Figs. 13a–c), significantly stronger than the normalized anomalies in the heavy composite (Figs. 5a–c), was present during much of the 30 December 1996–2 January 1997 event and during the two 1995 multiday events (not shown). The similar natures of the anomalies and the scales of the associated 700- and 500-hPa troughs during these separate events raise the question of whether the mul-

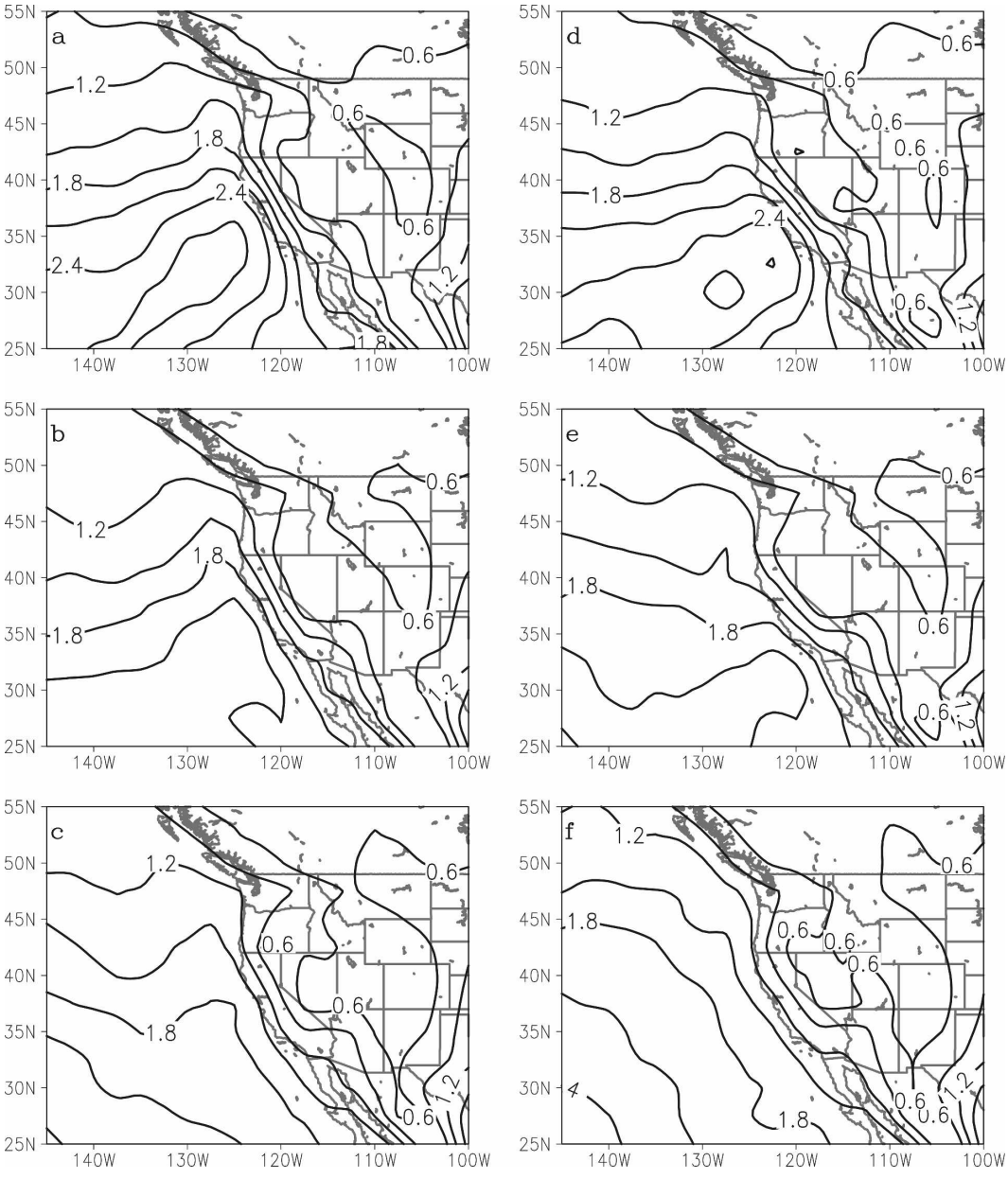

FIG. 11. Same as in Fig. 4, but for the composite mean PW (contour interval = 0.3 cm).

tiday extreme rainfall events may typically be associated with larger-scale negative geopotential 700- and 500-hPa (not shown) height anomalies than those corresponding to a 4-in. or greater event that lasts only 1 day. Visual inspection of several single-day rainfall events suggests this may be true; however, additional research is necessary.

The strong negative height anomaly and the presence of a weak positive anomaly to its southeast near Baja act to provide a strong gradient across northern California (Fig. 13). This combination helps explain the strong anomaly of the u and v wind components (not shown) at 700 hPa that was present throughout each of the three multiday events.

The 30 December 1996–2 January 1997 multiday event also was associated with anomalously strong 850-hPa winds (Fig. 14), with the westerly u component of the wind exhibiting an anomaly of greater than 3σ west of the California coast. The axis of the strongest 850-hPa winds remained aimed at northern California from 1200 UTC 30 December 1996 through 1200 UTC 1 January 1997. The 24-h accumulated rainfall maximum

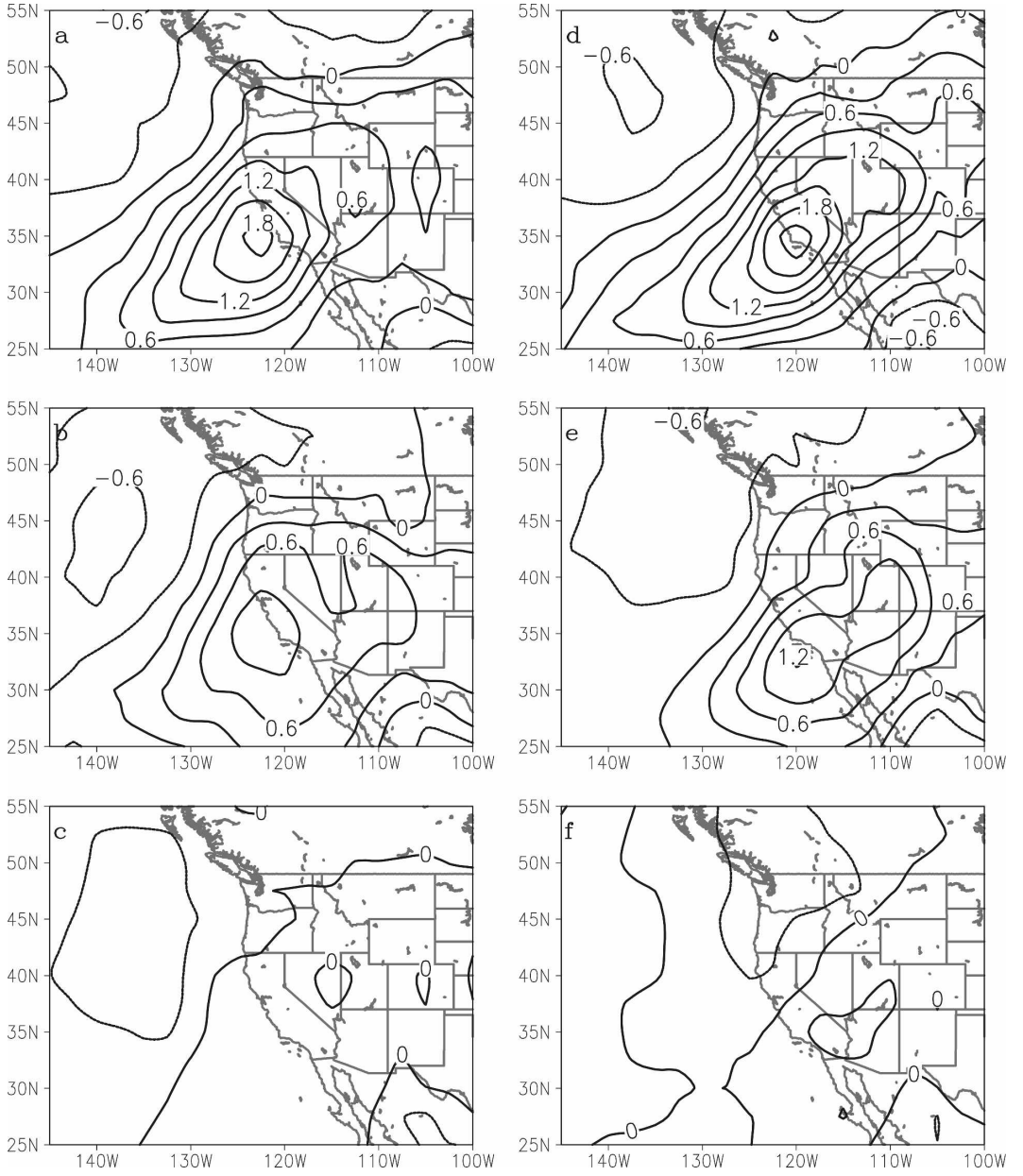

FIG. 12. Composite mean normalized anomaly of PW at $T + 00$ (beginning of heavy rainfall period) for the (a) heavy and (b) moderate rainfall groups, and $T + 24$ (end of period) for the (c) heavy and (d) moderate rainfall groups. Contour interval is 0.3σ.

for the two days ending at 1200 UTC January 1 was located north of San Francisco (Figs. 15a and 15b). The axis of the strongest 850-hPa winds sagged south through San Francisco later on 1–2 January, helping to explain the southward shift of the precipitation maximum valid at 1200 UTC 2 January 1997 (Fig. 15c).

The locations of the rainfall maxima over the Siskiyou range of northern California on 31 December 1996–1 January 1997 (Figs. 15a and 15b) are interesting to note. The strong southerly wind component (Fig. 16) over California at 850 hPa may help explain why there is a rainfall maximum in the Siskiyou Mountains at the northern end of the Sacramento Valley. Such a strong v wind component would help pull moisture northward up the valley and should contribute to enhanced lifting and rainfall along the southern facing slopes of the mountains. A similar rainfall maximum was observed during the 24-h periods ending at 1200 UTC on 9–10 January 1995 and 10–11 March 1995 (not shown).

The normalized anomaly fields were also plotted for

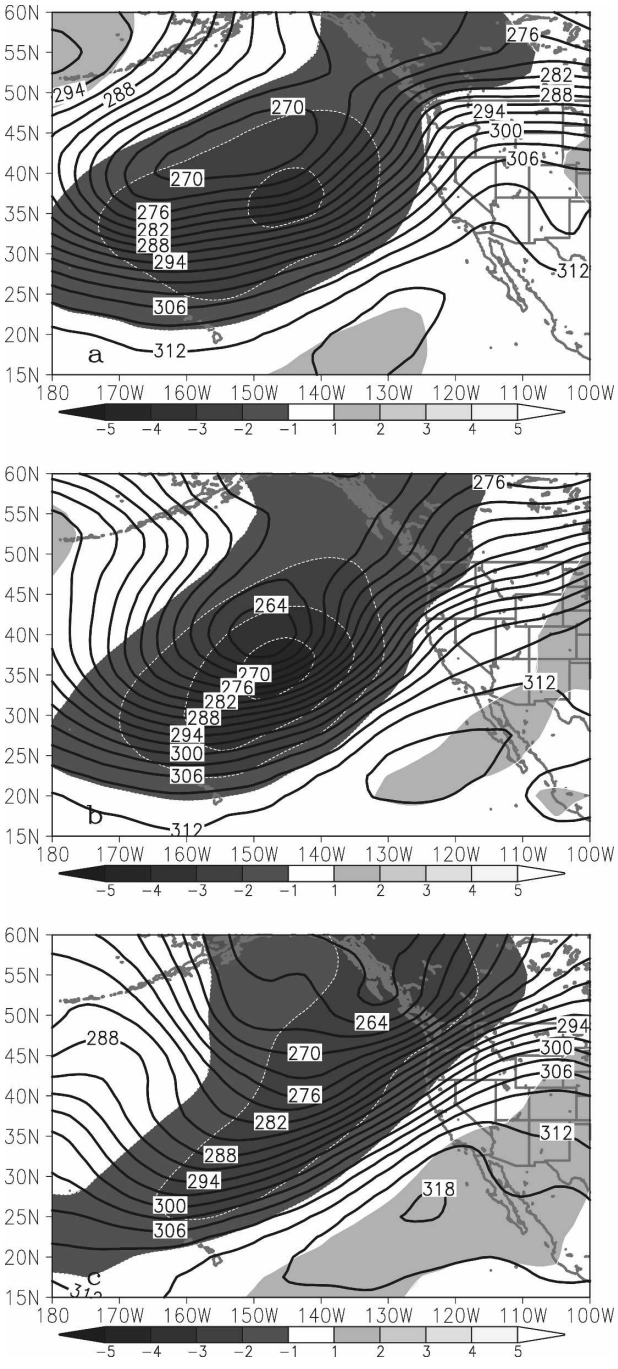

FIG. 13. The 700-hPa heights (dam) and normalized anomalies (shaded, contour interval = 1σ) at (a) 1200 UTC 30 Dec 1996, (b) 1200 UTC 31 Dec 1996, and (c) 1200 UTC 1 Jan 1997.

the magnitude of the total wind at 850 hPa (not shown) during the event, and compared with the anomalies of the u and v wind components. The normalized anomaly of the total wind may have given a slightly clearer signal of the system's rainfall potential than the anomaly field of either the u or v components of the wind. A fairly extensive normalized anomaly of greater than 3σ was present off the coast of California at 0000 UTC 31 December 1996 compared to a smaller area of normalized anomaly greater than 3σ for the u component of the wind. The normalized anomaly field of the total wind at 850 hPa at 0000 UTC 1 January 1997 had a larger area with an anomaly of greater than 4σ compared to the v-component wind anomaly field, but the maxima were centered in almost the same place (see Fig. 16b for the v-component anomaly center).

Neiman et al. (2002) found statistical links between observed rainfall rates and the measured hourly upslope component of the winds in the coastal mountain ranges of California. However, the authors pointed out that the relationship between upslope flow and precipitation is modulated on a case-by-case basis by a variety of factors that include moisture and thermodynamic stratification, the dynamics of the flow over and around terrain obstacles, latent heat release, and the efficiency of hydrometeor generation. The magnitude of the v-component anomalies implies that upslope is also important for modulating rainfall over the Siskiyou mountain range.

The 31 December 1996–2 January 1997 event was also associated with an atmospheric river that held a plume of anomalously high 850-hPa moisture flux (Fig. 17) and precipitable water (Fig. 18) that extended from near Hawaii into California. The anomalies for both fields exceeded 5σ, suggesting that this event was rare. Also, the width of the plume or river was wider than in the other two multiday events investigated and the areal coverage of the normalized anomalies was significantly larger than during any other case under review. The normalized anomalies during this event were significantly higher for the magnitude of the total moisture flux than for the magnitude of the total wind at 850 hPa (not shown), suggesting the former may provide a stronger signal for an impending extreme rainfall event.

The axis of the strongest moisture flux was aimed at California north of San Francisco during much of the 2 days ending at 12 UTC 1 January 1997 (Figs. 17a and 17b), which probably explains why the heaviest rainfall during those 2 days was located north of the city (Figs. 15a and 15b). The axis of MF started to shift back south to San Francisco by 1200 UTC 1 January 1997 (Fig. 17d) and by 0000 UTC 2 January 1997 (not shown) was clearly aimed south of the city. The area of maximum rainfall also shifted south (Fig. 15c) of San Francisco.

Reynolds (1996) studied three January and March 1995 multiday rainfall events and noted that during these particular major precipitation events, narrow intense bands of precipitation locked into terrain and produced heavy rain that led to flash flooding.

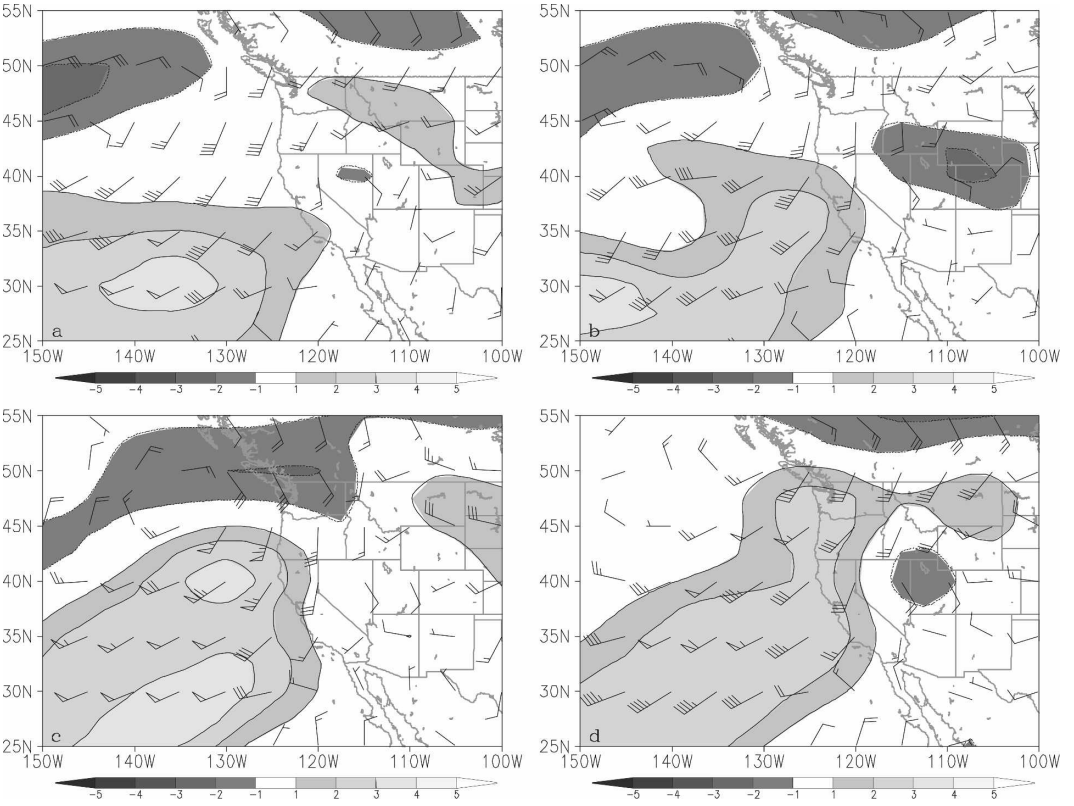

FIG. 14. The 850-hPa total wind (flags are 50 kt, barbs are 10 kt, and half barbs are 5 kt) and the normalized anomaly of the 850-hPa u component of the wind at (a) 1200 UTC 30 Dec 1996, (b) 0000 UTC 31 Dec 1996, (c) 0000 UTC 1 Jan 1997, and (d) 0000 UTC 2 Jan 1997. Magnitude of the normalized anomaly is shaded (contour interval = 1σ).

Inspection of the 850-hPa moisture flux anomalies and the observed precipitation indicated that the area where the precipitation was maximized during each day of these events coincided with the axis of highest moisture flux. One might conclude that the narrow bands of convection documented by Reynolds occurred within an axis of anomalously high 850-hPa moisture flux (not shown) during each case. While the widths of the bands of anomalously high 850-hPa moisture flux were thinner during the two 1995 events than the 1997 event, each 1995 event was associated with anomalously high 850-hPa moisture flux, with a portion of the band having more than 5σ above the normal moisture flux.

4. A determination of which fields have the highest correlation with the maximum observed rainfall in the Sierra Nevada range

The normalized anomaly of each of the parameters under review was positively correlated with the maximum precipitation contour analyzed in the Sierra Nevada range between 37.5° and 41.0°N for the values found at points 1 and 2 (Table 1). The highest R square was between the normalized anomaly of the magnitude of 700-hPa MF at point 1 and the analyzed precipitation maximum. The second highest R square was found with the component of the MF perpendicular to the Sierra range at 850 hPa at point 1. The R-square values between the normalized anomaly of the 850-hPa MF, the component of the 700-hPA perpendicular to the range at point 1, and the observed precipitation were almost as high. The R-square values for PW were also fairly high. The correlations between the u and v components of the wind at 850 and 700 hPa were lower than for PW or MF. The positive correlations between the various normalized anomalies associated with MF and PW are not surprising given the role that atmospheric rivers appear to have in delivering moisture to the West Coast during major cool season rainfall events.

It is worth noting that the Rhea orographic model (Pandey et al. 2000) uses 700-hPa winds for calculation of condensate supply rather than the 850-hPa winds, as the former have a higher correlation with precipitation.

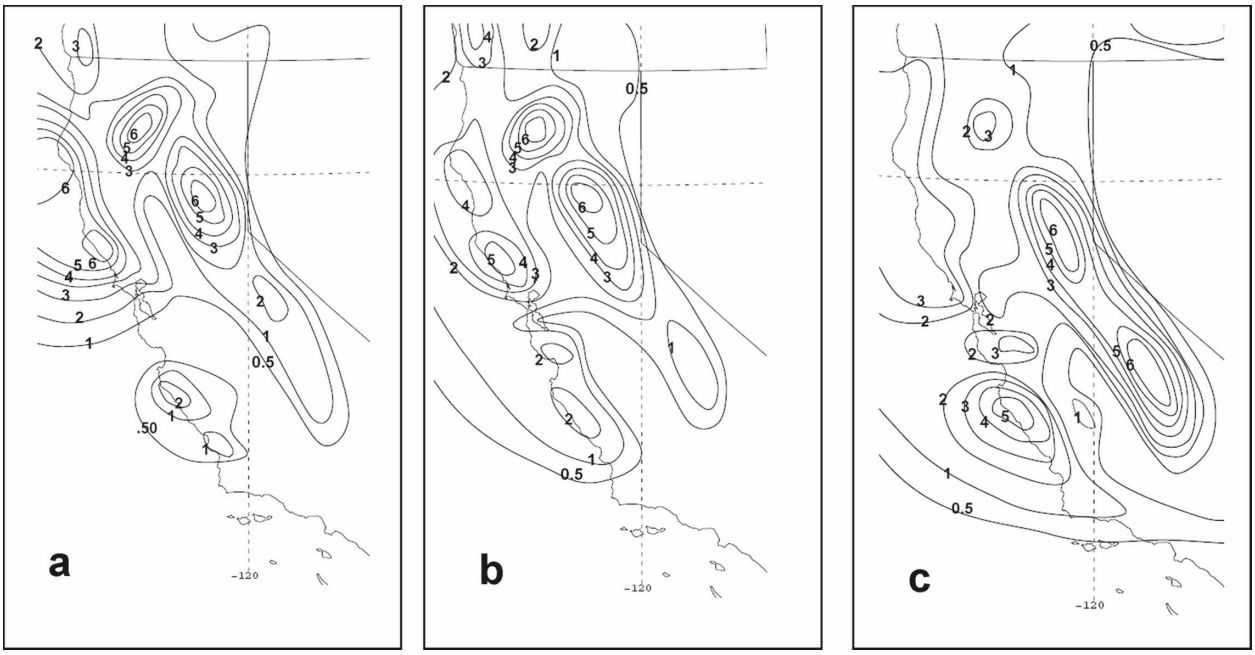

FIG. 15. HPC 24-h precipitation analyses valid at (a) 1200 UTC 31 Dec 1996, (b) 1200 UTC 1 Jan 1997, and (c) 1200 UTC 2 Jan 1997. Contour intervals are 0.50, 1.00, 2.00, 3.00, 4.00, 5.00, and 6.00 in.

Their correlations were developed with higher temporal resolution data than ours. Also, our correlations were with maximum rainfall analyzed anywhere along the Sierra range between 37.5° and 41.0°N while their correlations with rainfall were made using precipitation amounts that were much more site specific.

We also wanted to ascertain how common high normalized anomalies of 700- and 850-hPa MF (greater than 3σ) were at the point 37.5°N, 120°W when the negative 700-hPa height anomaly off the West Coast was also greater than 3σ. The combination of 700-hPa height and 850-hPa MF anomalies occurred only 26 times; both of these conditions were satisfied for the three multiday events noted above. All but 6 of these 26 events produced more than 4 in. of rainfall. Cases with normalized anomalies of at least 3σ in both the 700-hPa heights (off the California coast) and 700-hPa moisture flux (at 37.5°N, 120°W) were even more rare; only 16 cases satisfying these criteria were found. We conclude that the combination of normalized anomalies that was present during the three multiday events is relatively rare, supporting our contention that anomalies might be a valuable tool in forecasting multiday extreme rainfall events.

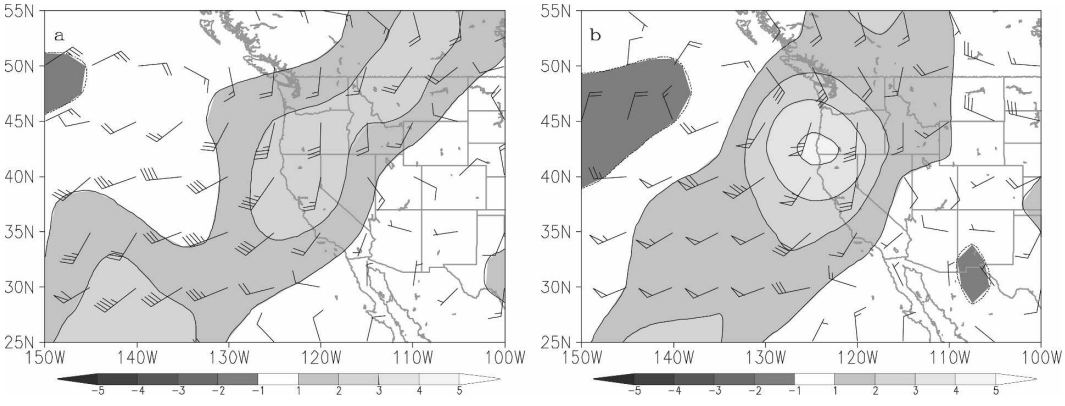

FIG. 16. The 850-hPa total wind (flags are 50 kt, barbs are 10 kt, and half barbs are 5 kt) and the normalized anomaly of the v component of the wind at (a) 0000 UTC 31 Dec 1996 and (b) 0000 UTC 1 Jan 1997. Magnitude of the normalized anomaly is shaded (contour interval = 1σ).

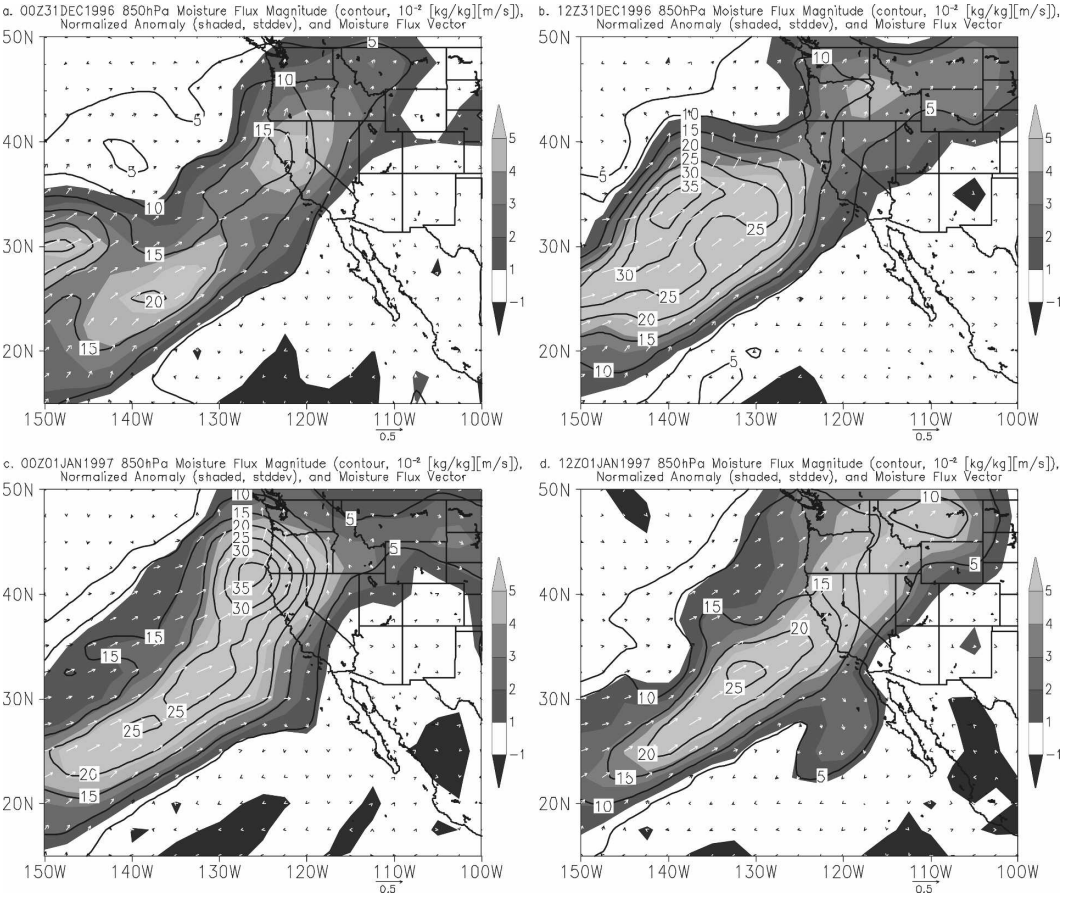

FIG. 17. The 850-hPA moisture flux (arrow; scale shown at bottom of figure), magnitude of MF (interval = 0.05 m s^{-1}) and the normalized anomaly of the moisture flux (magnitude of the anomaly is shaded with the scale on the right-hand side of the figure; interval is 1σ) at (a) 0000 UTC 31 Dec 1996, (b) 1200 UTC 31 Dec 1996, (c) 0000 UTC 1 Jan 1997, and (d) 1200 UTC 1 Jan 1997.

5. Conclusions

Based on the composite sample, a documentation of the synoptic-scale flow pattern accompanying extreme rainfall events over the mountains of northern California has been provided. The 500-hPa geopotential height anomalies found in the composite field indicate a southward shift of the polar jet in the east Pacific Ocean. The composites also reveal an area of negative height anomalies centered off the coast of northern California and/or southern Oregon from the surface to 500 hPa, and an area of positive anomalies located to the southeast of this center. Such an anomaly couplet virtually guarantees significantly stronger than normal geostrophic winds. Anomalously strong southerly and westerly wind components were present at the beginning of the period of heavy rainfall, with the southerly wind component anomaly extending southward into the subtropics, allowing subtropical moisture to be tapped. The stronger than normal southerly wind component also undoubtedly plays a role in supporting the anomalously warm air that typically accompanies the extreme rainfall events, and in the northward transport of moisture toward California via moisture plumes or atmospheric rivers.

The highest normalized anomalies found on the composites were for the fields of 850-hPa moisture flux and PW. The 850-hPa moisture flux anomaly was particularly noteworthy; all three multiday events had a moisture flux of at least 5σ greater than normal located within an atmospheric river off the coast. The three multiday events also were associated with a greater than 3σ negative departure from normal at 700 hPa. The combination of such a strong negative 700-hPa geopotential height anomaly and a strong MF anomaly is rare, suggesting that using these anomaly patterns may be useful when trying to predict a multiday extreme rainfall event.

The anomaly patterns for the three multiday events were very similar. All three events were associated with

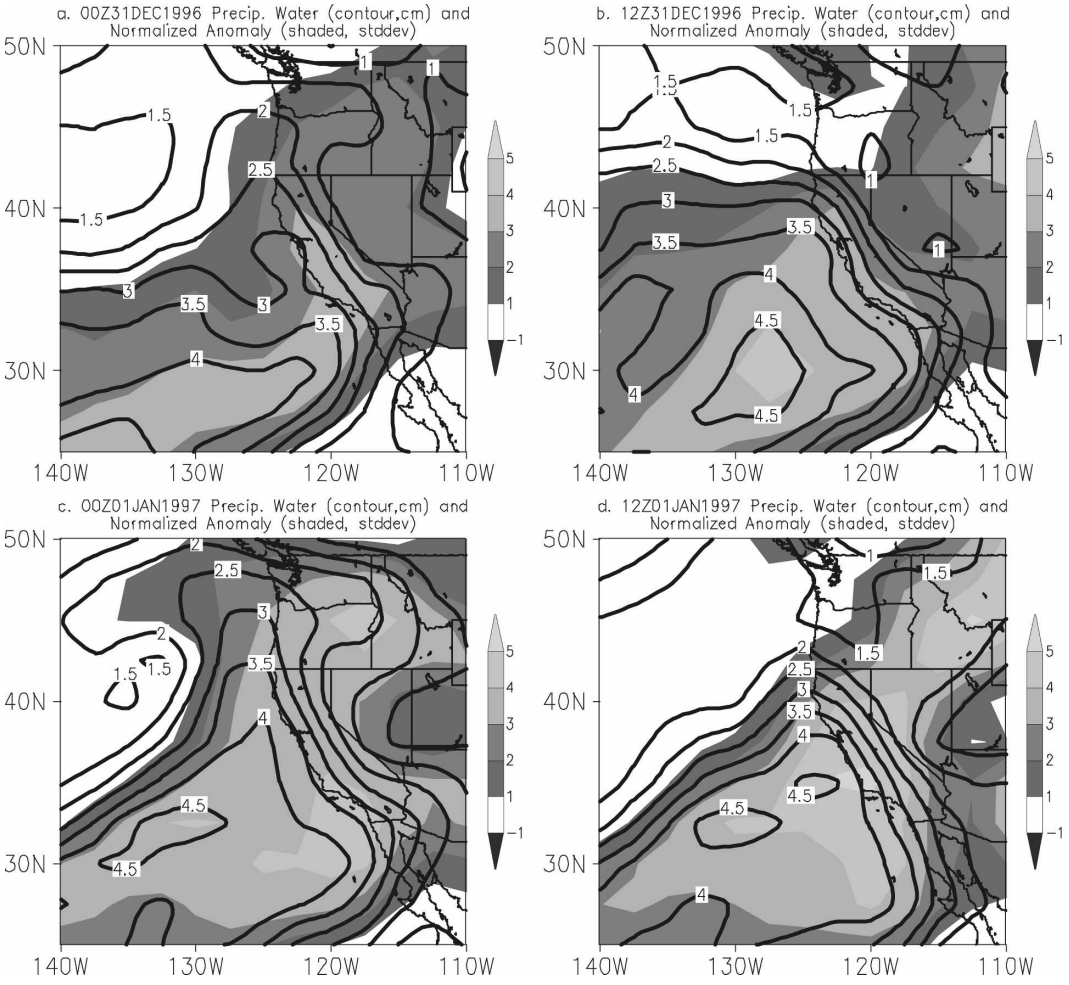

FIG. 18. The PW (contour interval = 0.5 cm) and normalized anomaly of PW at (a) 1200 UTC 30 Dec 1996, (b) 1200 UTC 31 Dec 1996, and (c) 1200 UTC 1 Jan 1997. Magnitude of the normalized anomaly (shaded); the scale is located on the right-hand side of the figure with an interval of 1σ.

700-hPa negative height anomalies greater than 3σ centered off the California coast, with a weaker positive anomaly to the southeast. Each event was also associated with anomalously strong 850-hPa winds, a plume of anomalously high PW indicative of an atmospheric river, and a plume of 850-hPa moisture flux with normalized anomalies greater than 4σ.

The similarities of the normalized anomalies during these events suggest that model forecasts of normalized anomalies of 700-hPa geopotential heights, 850-hPa winds, 850-hPa MF, and PW water may be useful in identifying extreme rainfall events providing that the models do a reasonable job at forecasting the synoptic pattern.

However, other factors need to be considered in addition to the normalized geopotential height, MF, wind, and PW anomaly patterns when predicting the expected magnitude and extent of the rainfall associated with a system approaching northern California, especially at the shorter time ranges; rainfall is modulated during each event by the atmospheric stability, the magnitude and extent of the synoptic and mesoscale forcing, the amount of latent heat release, and the efficiency of hydrometeor generation.

Beyond a day or two, models may not always have a good handle on many of these details but may still offer a useful depiction of the synoptic-scale anomaly patterns. Normalized anomalies derived from ensemble forecasts might offer insight into the probability of an extreme rainfall event occurring. Also, ensemble mean forecasts often have a better overall prediction of the synoptic-scale pattern than any single deterministic model. Because of the decreased resolution and impacts of the ensemble spread, ensemble mean forecasts usually will have smaller anomalies than those from deterministic forecasts from a single model. Therefore,

TABLE 1. *R*-square values calculated between the normalized anomaly values measured at point 1 (P1; 37.5°N, 120°W) and point 2 (P2; 35°N, 125°W) and the maximum analyzed rainfall contour found in the Sierra Nevada between 37.5° and 41.0°N on the official HPC precipitation analysis.

Parameter	*R* square (P1)	*R* square (P2)
850-hPa MF	0.52	0.50
700-hPa MF	0.59	0.47
700-hPa component of MF perpendicular to the Sierra Range	0.51	0.40
850-hPa component of MF perpendicular to the Sierra range	0.54	0.43
PW	0.48	0.40
700-hPa *u* component	0.25	0.22
700-hPa *v* component	0.15	0.24
850-hPa *u* component	0.07	0.28
850-hPa *v* component	0.32	0.28

if an ensemble mean forecasts normalized anomalies of greater than 3σ, there probably is a fairly high probability of an extreme rainfall event occurring.

Future research might concentrate on investigating how well the current generation of operational numerical models simulates moisture flux and PW within an atmospheric river. HPC now has normalized anomalies of various geopotential heights, PW, and the 850-hPa total wind and moisture flux available on their NCEP Advanced Weather Interactive Processing System (N-AWIPS) workstations and online (http://www.hpc.ncep.noaa.gov/training/SDs/). The HPC Web site is not supported operationally, so expect occasional interruptions of the data. The anomaly fields on the workstation and Web site are generated using the 1200 and 0000 UTC runs of the Global Forecast System (GFS), North American Mesoscale Model (NAM), and Short-Range Ensemble Forecast (SREF) mean output. Forecasters are currently evaluating the utility of normalized anomaly fields for improving their forecasts of extreme rainfall events over northern California.

Acknowledgments. The authors are grateful to Mr. Michael Bodner and Mr. Peter Manousos for their comprehensive reviews of the paper, and to Dr. James Hoke and Mr. Edwin Danaher for their support of the research.

REFERENCES

Alpert, P., 1986: Mesoscale indexing of the distribution of orographic precipitation over the high mountains. *J. Climate Appl. Meteor.,* **25,** 532–545.

——, and H. Shafir, 1991: Role of detailed wind–topography interaction in orographic rainfall. *Quart. J. Roy. Meteor. Soc.,* **117,** 421–426.

Army Corps of Engineers, 1999: Post-flood assessment for 1983, 1986, 1995, and 1997 in the Central Valley, California. The Army Corps of Engineers' Sacramento and San Joaquin River Basins Comprehensive Study, 48 pp. [Available online at http://www.spk.usace.army.mil/projects/civil/compstudy/docs/post_flood/START.pdf.]

Baird, B. P., and R. R. Robles, 1997: Emergency management issues in the California floods of 1997: Lessons learned or lessons lost? California Specialized Training Institute Doc. G4173 N3, San Luis Obispo, CA, 54 pp. [Available from California Specialized Training Institute, P.O. Box 8123, San Luis Obispo, CA 93403-8123.]

Cayan, D. R., and L. G. Riddle, 1993: Atmospheric circulation and precipitation in the Sierra Nevada. *Managing Water Resources During Global Change,* R. Herrman, Ed., American Water Resources Association, 711–719.

Faber, B. E., 2003: The potential for adaptive reservoir operations provided by forecast operations. *Proc. 2003 California Weather Symp.,* Sacramento, CA, CALFED Bay-Delta Program, 24–42. [Available from College of Natural Sciences and Mathematics, California State University, Sacramento, CA 95819.]

Ferraro, R. R., S. J. Kusselson, and M. Colton, 1998: An introduction to passive microwave remote sensing and its application to meteorological analysis and forecasting. *Natl. Wea. Dig.,* **22** (3), 11–23.

Grumm, R. H., and R. Hart, 2001a: Anticipating heavy rainfall: Forecast aspects. Preprints, *Symp. on Precipitation Extremes: Prediction, Impacts, and Responses,* Albuquerque, NM, Amer. Meteor. Soc., 66–70. [Available online at http://ams.confex.com/ams/annual2001/techprogram/paper_17422.htm.]

——, and ——, 2001b: Standardized anomalies applied to significant cold season weather events: Preliminary findings. *Wea. Forecasting,* **16,** 736–754.

——, N. W. Junker, R. Hart, and L. F. Bosart, 2002: Can possible heavy rainfall events be identified by comparing various parameters to climatological norms? Preprints, *19th Conf. on Weather Analysis and Forecasting,* San Antonio, TX, Amer. Meteor. Soc., 168–171. [Available online at http://ams.confex.com/ams/pdfpapers/47336.pdf.]

Hart, R., and R. H. Grumm, 2001: Using normalized climatological anomalies to rank synoptic-scale events objectively. *Mon. Wea. Rev.,* **129,** 2426–2442.

Holton, H. R., 2004*: An Introduction to Dynamic Meteorology.* 4th ed. Academic Press, 535 pp.

James, C. N., and R. A. Houze, 2005: Modification of precipitation by orography in storms crossing northern California. *Mon. Wea. Rev.,* **133,** 3110–3131.

Junker, N. W., R. H. Grumm, R. Hart, and L. F. Bosart, 2002: Establishing a 10 year climatology of 101.6 mm (4-inch) rainfall days, Part I. Preprints, *19th Conf. on Weather Analysis and Forecasting,* San Antonio, TX, Amer. Meteor. Soc., 156–159. [Available online at http://ams.confex.com/ams/pdfpapers/94229.pdf.]

Kalnay, E., and Coauthors, 1996: The NCEP/NCAR 40-Year Reanalysis Project. *Bull. Amer. Meteor. Soc.,* **77,** 437–471.

Kistler, R., and Coauthors, 2001: The NCEP–NCAR 50-Year Reanalysis: Monthly means CD-ROM and documentation. *Bull. Amer. Meteor. Soc.,* **82,** 247–267.

Lackmann, G. M., and J. R. Gyakum, 1999: Heavy cold-season precipitation in the northwestern United States: Synoptic climatology and an analysis of the flood of 17–18 January 1986. *Wea. Forecasting,* **14,** 687–700.

Maddox, R. A., F. Canova, and L. R. Hoxit, 1980: Meteorological characteristics of flash flood events over the western United States. *Mon. Wea. Rev.,* **108,** 1866–1877.

McDonald, B. E., T. M. Graziano, and C. K. Kluepfel, 2000: The NWS national QPF verification program. Preprints, *15th Conf. on Hydrology,* Long Beach, CA, Amer. Meteor. Soc., 247–250. [Available online at http://ams.confex.com/ams/annual2000/techprogram/paper_6441.htm.]

Neiman, P. J., F. M. Ralph, A. B. White, D. E. Kingsmill, and P. O. G. Perrson, 2002: The statistical relationship between upslope flow and rainfall in California's coastal mountains: Observations during CALJET. *Mon. Wea. Rev.,* **130,** 1468–1492.

——, ——, G. A. Wick, J. D. Lundquist, and M. D. Dettinger, 2008: Meteorological characteristics and overland precipitation impacts of atmospheric rivers affecting the west coast of North America based on eight years of SSMI/I satellite observations. *J. Hydrometeor.,* **9,** 22–47.

Pandey, G. R., D. R. Cayan, and K. P. Georgakakos, 1999: Precipitation structure in the Sierra Nevada of California during winter. *J. Geophys. Res.,* **104** (D10), 12 019–12 030.

——, ——, M. D. Dettinger, and K. P. Georgakakos, 2000: A hybrid orographic plus statistical model for downscaling precipitation in northern California. *J. Hydrometeor.,* **1,** 491–506.

Ralph, F. M., P. J. Neiman, and G. A. Wick, 2004: Satellite and CALJET aircraft observations of atmospheric rivers over the eastern North Pacific Ocean during the winter of 1997/1998. *Mon. Wea. Rev.,* **132,** 1721–1745.

——, ——, and R. Rotunno, 2005: Dropsonde observations in low-level jets over the northeastern Pacific Ocean from CALJET-1998 and PACJET-2001: Mean vertical-profile and atmospheric river characteristics. *Mon. Wea. Rev.,* **133,** 889–910.

——, ——, G. A. Wick, S. I. Gutman, M. D. Dettinger, D. R. Cayan, and A. B. White, 2006: Flooding on California's Russian River: Role of atmospheric rivers. *Geophys. Res. Lett.,* **33,** L13801, doi:10.1029/2006GL026689.

Reynolds, D. W., 1996: Similarities of three major precipitation events in California during 1995. Preprints, *15th Conf. on Weather Analysis and Forecasting,* Norfolk, VA, Amer. Meteor. Soc., J127–J130.

Rhea, J. O., 1978: Orographic precipitation model for hydrometeorological use. Ph.D. dissertation, Dept. of Atmospheric Science Paper 287, Colorado State University, Fort Collins, CO, 198 pp.

Strobin, M. H., and D. W. Reynolds, 1995: Forecasting hydrologically critical storms in northern and central California. Western Region Technical Attachment 95-22, 9 pp. [Available form NOAA/National Weather Service Western Region Headquarters, 125 South State St., Salt Lake City, UT 84103.]

Washburn, T., 2003: Connecting the dots: Fish, groundwater, and weather. *Proc. 2003 California Weather Symp.,* Sacramento, CA, CALFED Bay-Delta Program, 5–16. [Available from College of Natural Sciences and Mathematics, California State University, Sacremento, CA 95819.]

Zhu, Y., and R. E. Newell, 1998: A proposed algorithm for moisture fluxes from atmospheric rivers. *Mon. Wea. Rev.,* **126,** 725–735.